Letter

Room-Temperature van der Waals Perpendicular Ferromagnet Through Interlayer Magnetic Coupling

Yi Cao,[1,2,†] Xiaomin Zhang,[1,3,†] Xian-Peng Zhang,[4,5,†] Faguang Yan,[1] Ziao Wang,[1,3] Wenkai Zhu,[1,3] Hao Tan,[2] Vitaly N. Golovach,[5,6,7] Houzhi Zheng,[1,3] and Kaiyou Wang[1,2,3,*]

[1] *State Key Laboratory for Superlattices and Microstructures, Institute of Semiconductors, Chinese Academy of Sciences, Beijing 100083, China*

[2] *Beijing Academy of Quantum Information Sciences, Beijing 100193, China*

[3] *Center of Materials Science and Optoelectronic Engineering, University of Chinese Academy of Sciences, Beijing 100049, China*

[4] *Department of Physics, University of Basel, Klingelbergstrasse 82, 4056 Basel, Switzerland*

[5] *Donostia International Physics Center (DIPC), Manuel de Lardizabal 4, 20018 San Sebastian, Spain*

[6] *Centro de Fisica de Materiales (CFM-MPC), Centro Mixto CSIC-UPV/EHU, 20018 Donostia-San Sebastian, Basque Country, Spain*

[7] *IKERBASQUE, Basque Foundation for Science, 48011 Bilbao, Spain*

(Received 16 January 2022; revised 8 April 2022; accepted 8 April 2022; published 10 May 2022; corrected 12 January 2024)

Ferromagnetic van der Waals (vdW) crystals are promising for future spintronics because they hold huge potential in terms of tunable chemical, mechanical, and physical properties. However, room-temperature vdW ferromagnets with high-quality perpendicular magnetic anisotropy (PMA) are still elusive, limiting their practical implementations for spintronic applications, such as nonvolatile memories. Here, we show that the magnetic properties of vdW Fe_3GeTe_2, including the Curie temperature and the PMA, can be tuned by interlayer exchange coupling (IEC). We demonstrate strong ferromagnetic and antiferromagnetic IECs between sputtered Co and vdW Fe_3GeTe_2 with Pt and Ru spacer layers, respectively. We find that ferromagnetic IEC enhances the Curie temperature of Fe_3GeTe_2 while maintaining PMA, which can exhibit 100% out-of-plane remanent magnetization above room temperature. On the other hand, antiferromagnetic coupling weakens the PMA, resulting in a multilevel magnetic hysteresis loop of Fe_3GeTe_2 even at temperatures as small as 10 K. These interlayered coupled 3D/2D heterostructures could emerge as prime candidates for practical vdW spintronic applications.

DOI: 10.1103/PhysRevApplied.17.L051001

Introduction.—Due to the potential for stacking 2D spintronic heterostructures, room-temperature van der Waals (vdW) ferromagnets have long been desired by both the two-dimensional and the spintronics communities. Recently, intrinsic magnetism in vdW CrI_3, $Cr_2Ge_2Te_6$, Fe_3GeTe_2, etc., was discovered [1]. However, the Curie temperatures are far below room temperature for all these materials [2–4]. Since then, a variety of materials engineering approaches have been demonstrated to enhance the Curie temperatures. Approaches utilizing the electrostatic or ionic doping and/or gating effects [5–7], the size and shape effects [8], the interfacial spin-orbit coupling effect from topological insulators [9], and the proximity effects from antiferromagnets [10,11] have been demonstrated and examined. However, none of these works have reported a good perpendicular magnetic anisotropy (PMA) at room temperature, namely a typical rectangle magnetic hysteresis loop under an out-of-plane magnetic field, which is crucial for high-density nonvolatile spintronic applications.

In this work, we utilize interlayer exchange coupling (IEC) [12], an important concept that has been developed in early spintronics and applied in hard-disc read heads, to enhance the Curie temperature and PMA of vdW ferromagnets. Firstly, we theoretically demonstrate how the IEC from a high-Curie-temperature Co layer can influence the Curie temperature of a vdW material, such as Fe_3GeTe_2 (FGT). Then we experimentally verify the effects of ferromagnetic and antiferromagnetic IECs on the vdW ferromagnets by dry-transferring Fe_3GeTe_2 nanoflakes on sputtered Pt/Co/Pt and Pt/Co/Ru stacks, respectively.

Theory of curie-temperature regulation by IEC.—Theoretically, we study the effects of IEC on the magnetic properties of a low-Curie-temperature Fe_3GeTe_2 vdW nanoflake, which is indirectly coupled to a

*kywang@semi.ac.cn

†These authors contributed equally to this work.

high-Curie-temperature Co layer via a nonmagnetic Pt layer [see Figs. 1(a) and 1(b)]. The IEC arises from the Ruderman-Kittel-Kasuya-Yosida interaction between local moments on the FGT/Pt and Pt/Co interfaces across the Pt layer [13]. Here, we model the IEC as [13,14]

$$V = -\sum_{ij} J_{ij} S^i_{\mathrm{Fe}} \cdot S^j_{\mathrm{Co}}, \tag{1}$$

where J_{ij} is the IEC between the Co spin at site j, S^j_{Co}, and the Fe spin at site i, S^i_{Fe}. Although the interaction between PMA and IEC remains unclear in the Co/Pt/FGT trilayer [15,16], the PMA can be observed from a magnetic hysteresis loop [inset of Fig. 1(d)]. Hence, we calculate the magnetic field B and temperature T dependence of magnetization M. It can be derived from the Weiss mean-field approach, where the IEC amounts to a renormalization of the Weiss field:

$$H_{\mathrm{Fe}} = B - \frac{J_{\mathrm{Fe}}}{g\mu_B}\langle S_{\mathrm{Fe}}\rangle - \frac{J}{g\mu_B}\langle S_{\mathrm{Co}}\rangle . \tag{2}$$

Here g is the electron g-factor and μ_B is the Bohr magneton. The second term, an effective molecular field for ferromagnetism, is described by $J_{\mathrm{Fe}} = \sum_{i'} J_{ii'}$, where $J_{ii'}$ is the exchange coupling constant between spins S^i_{Fe} and $S^{i'}_{\mathrm{Fe}}$. The last term is an additional Weiss field from the IEC, with $J = \sum_j J_{ij}$. Though J_{ij} decays and oscillates with the distance between spins S^j_{Co} and S^i_{Fe} [Fig. 1(a)], we safely assume the same J for Fe spins in the FGT when the thickness of FGT, d_{FGT}, is much smaller than the oscillation period (I and II). Thus, J decays and oscillates with the thickness of the nonmagnetic Pt layer, d_{NM} [13]. The spin expectations can be derived from a partition function:

$$Z_{\mathrm{Fe}} = \sum_{S=-S_{\mathrm{Fe}}}^{S_{\mathrm{Fe}}} e^{-\beta g\mu_B S + \beta D_{\mathrm{Fe}} S^2}, \tag{3}$$

with $\beta = 1/k_B T$. Here, we include a local axial magnetic anisotropy energy $-D_{\mathrm{Fe}}\sum_i (S^{i,z}_{\mathrm{Fe}})^2$ and omit the magnetostatic and magnetoelastic energies for simplicity [17].

The effect of the Co layer on the FGT nanoflake can be understood qualitatively on the basis of the three-spin exchange among Co and Fe spins, as plotted in Fig. 1(b). For uniform IEC, J_{ij} (I and II), two Fe spins

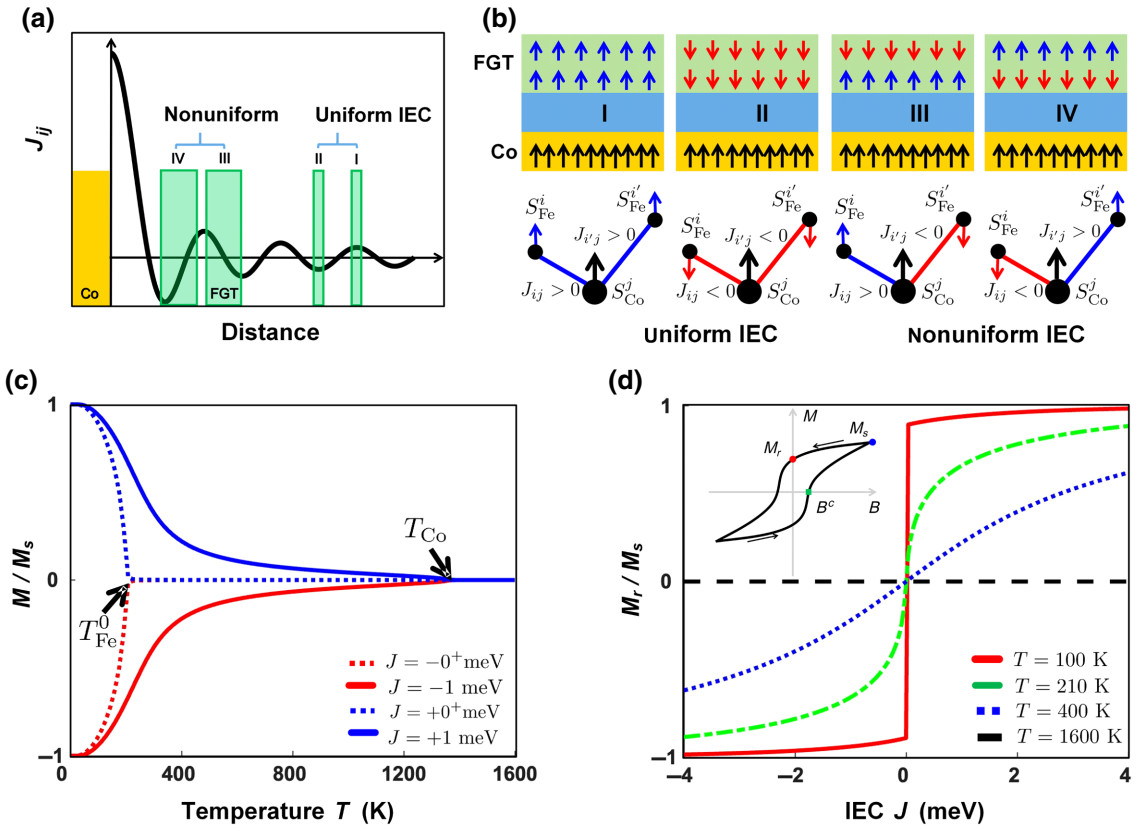

FIG. 1. Equilibrium spin orientations and expectations in a Co/Pt/FGT trilayer with IEC. (a) IEC J_{ij} as a function of the distance between two localized spins. It depends on the thicknesses of both nonmagnetic layer and FGT, d_{NM} and d_{FGT}. (b) Relative spin orientations and three-spin exchange among Co and Fe spins at weak magnetic fields. (c) Magnetization M as a function of temperature T for different IECs. T^0_{Co} and T_{Co} are Curie temperatures of FGT nanoflake and Co layer in the absence of the IEC, respectively. (d) Remanent magnetization M_r as a function of the IEC J for different T. The inset shows a magnetic hysteresis loop with coercive field B^c, saturation magnetization M_s, and remanent magnetization M_r.

S^{i}_{Fe} and $S^{i'}_{\mathrm{Fe}}$ always prefer a ferromagnetic order, because the IECs J_{ij} and $J_{i'j}$ have the same sign. Thus, both ferromagnetic and antiferromagnetic IECs contribute to the ferromagnetic order between two Fe spins of FGT, as shown in Fig. 1(b). Next, we discuss quantitatively the magnetization. For ferromagnetic (antiferromagnetic) IEC, $\langle S_{\mathrm{Fe}}\rangle$ has the same (different) sign as $\langle S_{\mathrm{Co}}\rangle$ as shown in I (II) of Fig. 1(b). Hence, the Weiss field acting on Fe spins is enhanced due to the IEC. The Co layer with a much higher Curie temperature stabilizes the magnetic order in FGT beyond the Curie temperature of the FGT itself, T^{0}_{Fe}. This explains the enhancement of T_{Fe}, as plotted in Fig. 1(c). Besides, Fig. 1(d) plots remanent magnetization M_r as a function of J for different T. For high enough temperatures ($T > T^{0}_{\mathrm{Co}}$), the IEC Weiss field, proportional to $\langle S_{\mathrm{Co}}\rangle$, is zero and hence $M_r = 0$. For $T^{0}_{\mathrm{Fe}} < T < T^{0}_{\mathrm{Co}}$, S_{Co} is nonzero and M_r is positive and negative for ferromagnetic and antiferromagnetic IECs, respectively. There exists a gap for temperature $T < T^{0}_{\mathrm{Fe}}$, accounting for M_r of FGT itself. It is enhanced by the IEC, because both ferromagnetic and antiferromagnetic IECs provide an additional contribution to ferromagnetic order [I and II of Fig. 1(b)]. In summary, both ferromagnetic and antiferromagnetic IECs lead to the enhancement of the Curie temperature and PMA of the FGT.

Observation of curie-temperature enhancement by ferromagnetic IEC.—In order to create a structure with IEC, Fe_3GeTe_2 nanoflake is dry-transfered onto a sputtered Ta(1)/Pt(4)/Co(0.5)/Pt(0.4) (thickness in nm, referred to as PCP, the substrate is Si(0.5 mm)/SiO_2(300 nm) wafer) 6-μm-width Hall bar device, as shown schematically in Fig. 2(a). Note that this configuration is different from that for most of previously reported Hall measurements of Fe_3GeTe_2/Pt heterostructures, where the Pt layer is deposited onto the vdW Fe_3GeTe_2 surface [18,19]. A high-quality Pt/Fe_3GeTe_2 interface is obtained, confirming by the typical rectangle-shaped magnetic hysteresis loops (represented by R_H-B_z loops, i.e., anomalous Hall resistance versus out-of-plane magnetic field) observed from a Ta(1)/Pt(4)/Fe_3GeTe_2 (thickness in nm) reference sample [20], whose Curie temperature is read to be between 210 and 230 K, consistent with previous literature [1]. An optical image of the device and height profile of the FGT are shown in Figs. 2(b) and 2(c), respectively.

Accordingly, for the PCP/FGT sample with two individual ferromagnetic components, the expected steplike R_H-B_z loops are observed at various temperatures [20]. Due to the current shunting effect of the conductive Fe_3GeTe_2, as illustrated in Fig. 2(d), the measured R_H of the PCP/FGT sample should be smaller than that of the PCP sample when the temperature T is above the Curie temperature T_C of Fe_3GeTe_2, i.e., $(T > T_C) \Rightarrow (R_H^{\mathrm{PCP/FGT}} < R_H^{\mathrm{PCP}})$. The contrapositive equivalent of the above statement is $(R_H^{\mathrm{PCP/FGT}} > R_H^{\mathrm{PCP}}) \Rightarrow (T < T_C)$, i.e., if $R_H^{\mathrm{PCP/FGT}} > R_H^{\mathrm{PCP}}$, then one can conclude that Fe_3GeTe_2 is below its T_C and retains PMA. This is exactly the case for the PCP/FGT sample, as shown in Fig. 2(e), where much larger $R_H^{\mathrm{PCP/FGT}}$ compared with R_H^{PCP} are observed at all measured temperatures from 10 to 310 K. Remarkably, Fig. 2(f) shows a typical rectangle-shaped (though steplike) R_H hysteresis loop of the PCP/FGT sample even at 310 K, which clearly indicates a sufficient PMA of the transferred Fe_3GeTe_2 nanoflake with 100% out-of-plane magnetic remanence above room temperature. Furthermore, as shown in Fig. 2(f), all switching steps on the R_H-B_z loop of the PCP/FGT sample show obvious larger coercive field than that of the PCP sample at 310 K, suggesting strong ferromagnetic IEC between the sputtered Co layer and the transferred vdW Fe_3GeTe_2 nanoflake.

Observation of PMA reduction by antiferromagnetic IEC.—A Ru spacer layer usually gives rise to antiferromagnetic IEC between two ferromagnets. To experimentally achieve this, we transfer the Fe_3GeTe_2 nanoflake onto Pt/Co/Ru Hall bars. One expects the negative remanent magnetization and the enhanced Curie temperature and PMA as discussed in Sec. II. However, it has totally different behavior. Figure 3(a) shows the hysteresis loops of the Ta(1)/Pt(4)/Co(0.5)/Ru(0.4)/Fe_3GeTe_2 sample (referred to as PCR/FGT) at various temperatures [20]. Clear antiferromagnetic coupling behaviors with two sharp switching steps are found, where the first switching step shows a negative coercivity. By referring to the hysteresis loops of reference Ta(1)/Pt(4)/Co(0.5)/Ru(0.4) samples (referred to as PCR) [20], the Co always exhibits binary magnetization states with very sharp switching behaviors. Therefore, the second sharp switching step in Fig. 3(a) is determined as the switching of the Co layer, and thereby the first sharp switching step and the gradual multilevel switching parts are the switching of Fe_3GeTe_2. Note that an Fe_3GeTe_2 nanoflake usually shows strong PMA at low temperatures with rectangular magnetic hysteresis loops [20], which are in great contrast to the PCR/FGT sample, as shown in Fig. 3(a). By extracting the Fe_3GeTe_2 component of the total hysteresis loop [see Fig. 3(b)], the perpendicular magnetic remanence and the saturation magnetic field of Fe_3GeTe_2 are obtained, as shown in Figs. 3(c) and 3(d), respectively. The remanence is positive, rather the negative remanence shown in Fig. 1(d). Even at 10 K, the Fe_3GeTe_2 nanoflake exhibits low remanence (18.3%) and considerable saturation magnetic field (0.174 T), indicating a weak PMA of the Fe_3GeTe_2 nanoflake when it is in antiferromagnetic coupling with the Co layer.

Discussion.—First, we try to qualitatively explain the PMA reduction from the nonuniform IEC. When d_{FGT} is of the order of the oscillation period, our previous assumption of the uniform IEC fails, and the IEC changes layer

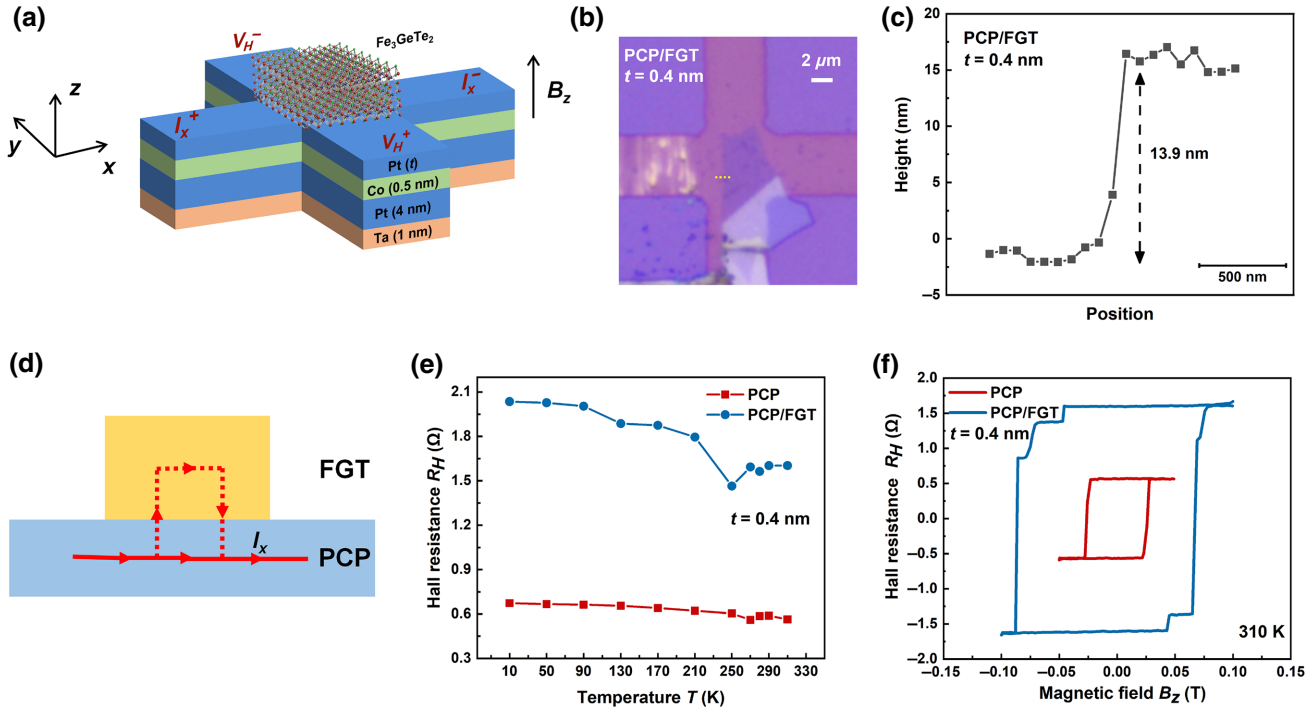

FIG. 2. Magnetic properties of Ta(1)/Pt(4)/Co(0.5)/Pt(0.4) (thickness in nm, referred to as PCP) and Ta(1)/Pt(4)/Co(0.5)/Pt(0.4)/Fe_3GeTe_2 (referred to as PCP/FGT) samples. (a) Schematic of the device structure and the Hall measurements. The Hall resistance R_H is obtained by dividing the measured Hall voltage V_H by the applied channel current (100 μA). (b) Optical image of the PCP/FGT sample. (c) Height profile along the dashed line measured by atomic force microscopy. (d) Schematic illustration of the current shunting effect. (e) Hall resistance R_H as a function of temperature T. (f) Hall resistance R_H versus out-of-plane magnetic field B_z.

by layer, as shown in Fig. 1(a) (III and IV). The first sharp switching has a negative coercivity [Fig. 3(a)], corresponding to the spin flips of some layers with antiferromagnetic IEC. Thus, the FGT nanoflake is divided into two zones with opposite spins as plotted in Fig. 1(b) (III and IV). The gradual switching is linear, implying antiferromagnetic multilayers [21]. In our case, this might result from the long-range antiferromagnetic order between different layers. By "long range," we mean the IEC can couple two Fe spins in different layers far away from each other via three-spin exchange [Fig. 1(b)]. For example, when d_{FGT} is large and the IEC varies from positive to negative, the three-spin exchange leads to antiferromagnetic order between two spins with different signs of IECs. Therefore, this behavior of sharp step plus gradual switching, as shown in Fig. 3(b), implies that the remanence does depend on the spatial distribution of IECs. A full sharp switching from uniform antiferromagnetic IEC definitely causes negative remanence [dashed-line loop of Fig. 3(e)]. But a small sharp switching from nonuniform IEC, followed by a long gradual switching, might result in positive remanence [solid-line loop of Fig. 3(e)]. This might explain the PMA reduction of FGT.

Besides, we fabricate more than 10 replicas for each of the above PCP/FGT and PCR/FGT samples; however, not all samples show good IEC and magnetic property changes. Besides the best samples shown in Figs. 2 and 3, there are also reproducible results exhibiting obvious ferromagnetic and antiferromagnetic IECs and thereby consistent changes in Curie temperature and PMA of Fe_3GeTe_2 [20], respectively. Nevertheless, this sample-to-sample variation indicates strict requirements for realizing sufficient IEC. One possible reason is the uncertain distance between the sputtered stack surface and the dry-transferred vdW nanoflakes, since it is well known that the spacer layer thickness is considered as an important factor for IEC [22]. Further experimental investigation with dedicated control of the Pt/Fe_3GeTe_2 interface is required, which is difficult at this stage. Even so, we can still attribute the observed Curie-temperature enhancement shown in Fig. 1 to the effect of IEC by excluding the proximity effect from the Co as well as the proximal magnetized upper Pt layers, since the proximity-induced magnetic moment in Pt is reported to decay exponentially with increasing distance from the Co/Pt interface within approximately 1 nm [23,24]. It should also be mentioned that the multilevel magnetized Fe_3GeTe_2 shown in Fig. 3(a) could potentially work as a vdW spintronic synapse for neuromorphic computing [25,26]. In the future, emerging high-Curie-temperature vdW materials, such as Fe_5GeTe_2 [27,28], can also be adopted into our IEC scheme for even higher performance, since

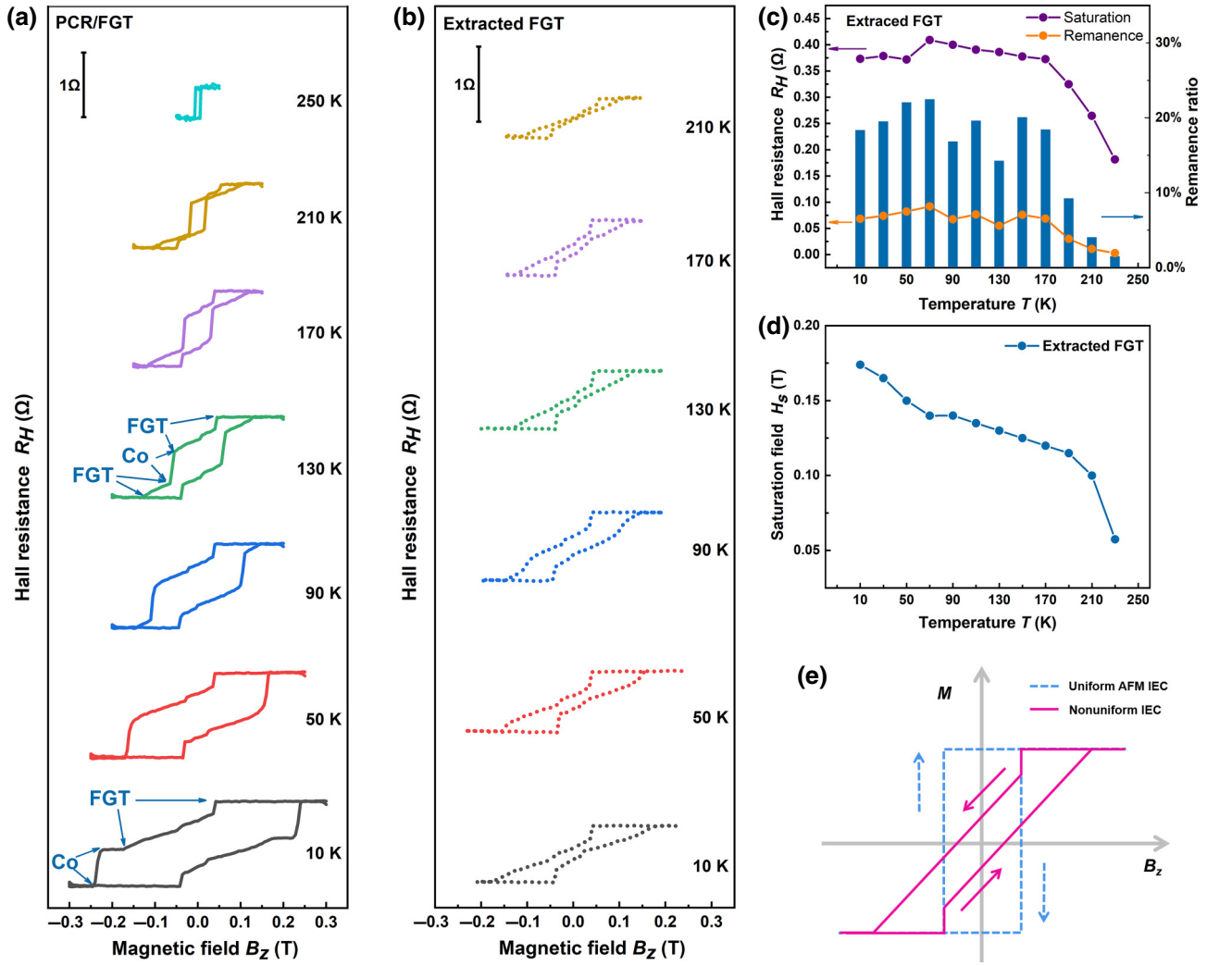

FIG. 3. Magnetic properties of Ta(1)/Pt(4)/Co(0.5)/Ru(0.4)/Fe_3GeTe_2 (referred to as PCR/FGT) sample. (a) R_H-B_z loops for the PCR/FGT sample at various temperatures. Taking 10 and 130 K as two examples, each switching part of Co and Fe_3GeTe_2 is marked on the loops. (b) Extracted R_H-B_z loops for FGT by manually subtracting the R_H contribution of Co from (a). (c) Saturation and remanence Hall resistances, and thereby the corresponding remanence ratio of Fe_3GeTe_2 extracted from (a) as a function of temperature T. (d) Saturation magnetic field of the extracted Fe_3GeTe_2 as a function of temperature T. (e) Schematic of the magnetic hysteresis loops of FGT under uniform antiferromagnetic IEC (blue dashed line) and nonuniform IEC (pink solid line).

practical nonvolatile memories are required to maintain PMA much above room temperature for better data retention.

Summary.—We study Curie temperature and PMA regulation of vdW Fe_3GeTe_2 by IEC both theoretically and experimentally. Ferromagnetic and antiferromagnetic IECs between the sputtered Co layer and the dry-transferred Fe_3GeTe_2 nanoflake are observed and discussed in structures with Pt and Ru spacer layers, respectively. We demonstrate above-room-temperature ferromagnetic vdW Fe_3GeTe_2 with 100% out-of-plane magnetization remanence in Pt/Co/Pt/Fe_3GeTe_2 samples with ferromagnetic IEC. For Pt/Co/Ru/Fe_3GeTe_2 samples with antiferromagnetic IEC, reduced PMA in the Fe_3GeTe_2 nanoflake with gradual multilevel switching behavior is observed even at 10 K. Our work opens up opportunities in applications of vdW ferromagnets with tunable Curie temperature and PMA, as well as explorations of emerging physics at a 3D/2D interface.

Acknowledgments.—This work is supported by the National Key R&D Program of China (Grant No. 2017YFA0303400), Beijing Natural Science Foundation Key Program (Grant No. Z190007), National Natural Science Foundation of China (Grants No. 62104018, No. 11474272, and No. 61774144), Chinese Academy of Sciences (Grants No. QYZDY-SSW-JSC020, No. XDB44000000, and No. XDB28000000), Beijing Natural Science Foundation (Grant No. 2212048), Swiss National Science Foundation and NCCR SPIN, and the Spanish Ministerio de Ciencia, Innovación y Universidades (MICINN) through Project PID2020-114252GB-I00 (SPIRIT).

[1] K. S. Burch, D. Mandrus, and J. Park, Magnetism in two-dimensional van der Waals materials, Nature **563**, 47 (2018).

[2] B. Huang, G. Clark, E. Navarro-Moratalla, D. R. Klein, R. Cheng, K. L. Seyler, D. Zhong, E. Schmidgall, M. A. McGuire, D. H. Cobden, W. Yao, D. Xiao, P. Jarillo-Herrero, and X. Xu, Layer-dependent ferromagnetism in a van der Waals crystal down to the monolayer limit, Nature **546**, 270 (2017).

[3] C. Gong, L. Li, Z. Li, H. Ji, A. Stern, Y. Xia, T. Cao, W. Bao, C. Wang, Y. Wang, Z. Q. Qiu, R. J. Cava, S. G. Louie, J. Xia, and X. Zhang, Discovery of intrinsic ferromagnetism in two-dimensional van der Waals crystals, Nature **546**, 265 (2017).

[4] Z. Fei, B. Huang, P. Malinowski, W. Wang, T. Song, J. Sanchez, W. Yao, D. Xiao, X. Zhu, A. F. May, W. Wu, D. H. Cobden, J. Chu, and X. Xu, Two-dimensional itinerant ferromagnetism in atomically thin Fe_3GeTe_2, Nat. Mater. **17**, 778 (2018).

[5] B. Huang, G. Clark, D. R. Klein, D. MacNeill, E. Navarro-Moratalla, K. L. Seyler, N. Wilson, M. A. McGuire, D. H. Cobden, D. Xiao, W. Yao, P. Jarillo-Herrero, and X. Xu, Electrical control of 2D magnetism in bilayer CrI_3, Nat. Nanotechnol. **13**, 544 (2018).

[6] S. Jiang, L. Li, Z. Wang, K. F. Mak, and J. Shan, Controlling magnetism in 2D CrI_3 by electrostatic doping, Nat. Nanotechnol. **13**, 549 (2018).

[7] Y. Deng, Y. Yu, Y. Song, J. Zhang, N. Z. Wang, Z. Sun, Y. Yi, Y. Z. Wu, S. Wu, J. Zhu, J. Wang, X. Chen, and Y. Zhang, Gate-tunable room-temperature ferromagnetism in two-dimensional Fe_3GeTe_2, Nature **563**, 94 (2018).

[8] Q. Li, *et al.*, Patterning-induced ferromagnetism of Fe_3GeTe_2 van der Waals materials beyond room temperature, Nano Lett. **18**, 5974 (2018).

[9] H. Wang, Y. Liu, P. Wu, W. Hou, Y. Jiang, X. Li, C. Pandey, D. Chen, Q. Yang, H. Wang, D. Wei, N. Lei, W. Kang, L. Wen, T. Nie, W. Zhao, and K. L. Wang, Above room-temperature ferromagnetism in wafer-scale two-dimensional van der Waals Fe_3GeTe_2 tailored by topological insulator, ACS Nano **14**, 10045 (2020).

[10] L. Zhang, X. Huang, H. Dai, M. Wang, H. Cheng, L. Tong, Z. Li, X. Han, X. Wang, L. Ye, and J. Han, Proximity-coupling-induced significant enhancement of coercive field and Curie temperature in 2D van der Waals heterostructures, Adv. Mater. **32**, 2002032 (2020).

[11] H. Idzuchi, A. E. L. Allcca, X. C. Pan, K. Tanigaki, and Y. P. Chen, Increased Curie temperature and enhanced perpendicular magneto anisotropy of $Cr_2Ge_2Te_6$/NiO heterostructure, Appl. Phys. Lett. **115**, 232403 (2019).

[12] S. S. P. Parkin, N. More, and K. P. Roche, Oscillations in Exchange Coupling and Magnetoresistance in Metallic Superlattice Structures: Co/Ru, Co/Cr, and Fe/Cr, Phys. Rev. Lett. **64**, 2304 (1990).

[13] A. Ney, F. Wilhelm, M. Farle, P. Poulopoulos, P. Srivastava, and K. Baberschke, Oscillations of the curie temperature and interlayer exchange coupling in magnetic trilayers, Phys. Rev. B **59**, R3938 (1999).

[14] P. Bruno and C. Chappert, Oscillatory Coupling Between Ferromagnetic Layers Separated by a Nonmagnetic Metal Spacer, Phys. Rev. Lett. **67**, 1602 (1991).

[15] J. Chen, S. Peng, D. Xiong, H. Cheng, H. Zhou, Y. Jiang, J. Lu, W. Li, and W. Zhao, Correlation of interfacial perpendicular magnetic anisotropy and interlayer exchange coupling in CoFe/W/CoFe structures, J. Phys. D: Appl. Phys. **53**, 334001 (2020).

[16] C. J. Aas, P. J. Hasnip, R. Cuadrado, E. M. Plotnikova, L. Szunyogh, L. Udvardi, and R. W. Chantrell, Exchange coupling and magnetic anisotropy at Fe/FePt interfaces, Phys. Rev. B **88**, 174409 (2013).

[17] M. Hoffmann, B. Zimmermann, G. P. Müller, D. Schürhoff, N. S. Kiselev, C. Melcher, and S. Blügel, Antiskyrmions stabilized at interfaces by anisotropic Dzyaloshinskii-Moriya interactions, Nat. Commun. **8**, 308 (2017).

[18] M. Alghamdi, M. Lohmann, J. Li, P. R. Jothi, Q. Shao, M. Aldosary, T. Su, B. P. T. Fokwa, and J. Shi, Highly efficient spin-orbit torque and switching of layered ferromagnet Fe_3GeTe_2, Nano Lett. **19**, 4400 (2019).

[19] X. Wang, *et al.*, Current-driven magnetization switching in a van der Waals ferromagnet Fe_3GeTe_2, Sci. Adv. **5**, eaaw8904 (2019).

[20] See Supplemental Material at http://link.aps.org/supplemental/10.1103/PhysRevApplied.17.L051001 for the temperature-dependent R_H-B_z loops for a Pt/FGT reference sample, two PCP/FGT samples, and two PCR/FGT samples.

[21] J. Seo, E. S. An, T. Park, S.-Y. Hwang, G.-Y. Kim, K. Song, W.-S. Noh, J. Y. Kim, G. S. Choi, M. Choi, E. Oh, K. Watanabe, T. Taniguchi, J.-H. Park, Y. J. Jo, H. W. Yeom, S.-Y. Choi, J. H. Shim, and J. S. Kim, Tunable high-temperature itinerant antiferromagnetism in a van der Waals magnet, Nat. Commun. **12**, 2844 (2021).

[22] P. Bruno, Theory of interlayer n1agnetic coupling, Phys. Rev. B **52**, 411 (1995).

[23] M. Suzuki, H. Muraoka, Y. Inaba, H. Miyagawa, N. Kawamura, T. Shimatsu, H. Maruyama, N. Ishimatsu, Y. Isohama, and Y. Sonobe, Depth profile of spin and orbital magnetic moments in a subnanometer Pt film on Co, Phys. Rev. B **72**, 054430 (2005).

[24] A. Mukhopadhyay, S. K. Vayalil, D. Graulich, I. Ahamed, S. Francoual, A. Kashyap, T. Kuschel, and P. S. A. Kumar, Asymmetric modification of the magnetic proximity effect in Pt/Co/Pt trilayers by the insertion of a Ta buffer layer, Phys. Rev. B **102**, 144435 (2020).

[25] Y. Cao, A. W. Rashforth, Y. Sheng, H. Zheng, and K. Wang, Tuning a binary ferromagnet into a multistate synapse with spin-orbit-torque-induced plasticity, Adv. Funct. Mater. **29**, 1808104 (2019).

[26] X. Lan, Y. Cao, X. Liu, K. Xu, C. Liu, H. Zheng, and K. Wang, Gradient descent on multilevel spin-orbit synapses with tunable variations, Adv. Intell. Syst. **3**, 2000182 (2021).

[27] H. Zhang, R. Chen, K. Zhai, X. Chen, L. Caretta, X. Huang, R. V. Chopdekar, J. Cao, J. Sun, J. Yao, R. Birgeneau, and R. Ramesh, Itinerant ferromagnetism in van der Waals $Fe_{5-x}GeTe_2$ crystals above room temperature, Phys. Rev. B **102**, 064417 (2020).

[28] A. F. May, D. Ovchinnikov, Q. Zheng, R. Hermann, S. Calder, B. Huang, Z. Fei, Y. Liu, X. Xu, and M. A. McGuire, Ferromagnetism near room temperature in the cleavable van der Waals crystal Fe_5GeTe_2, ACS Nano **13**, 4436 (2020).

Correction: A typographical error in the third affiliation has been fixed.